Structural Analyses of Apricot Pectin Polysaccharides by NMR Spectroscopy

Zayniddin Kamarovich Muhidinov *, Matlub H. Rahmonov, Abduvaly Jonmurodov, Jamshed Bobokalonov, Lin Shu Liu *, Gary Strahan

Posted Date: 4 December 2023

doi: 10.20944/preprints202312.0151.v1

Keywords: apricot pectin; NMR spectroscopy; RG-I; HG; RG-II; arabinogalactan; molecular weight; conformation

Article

Structural Analyses of Apricot Pectin Polysaccharides by NMR Spectroscopy

Zayniddin K. Muhidinov [1,*], Matlub H. Rahmonov [1], Abduvaly S. Jonmurodov [1], Jamshed T. Bobokalonov [1], Gary D. Strahan [2] and Lin Shu Liu [2,*]

[1] Chemistry Institute of the National Academy of Sciences of Tajikistan, 299/2 Ainy str., Dushanbe 734063, Tajikistan; muhidinovzayniddin@gmail.com

[2] Eastern Regional Research Center of the ARS USDA, Wyndmoor 19038 USA; linshu.liu@usda.gov

* Correspondence: muhidinovzayniddin@gmail.com; linshu.liu@usda.gov

Abstract: The fine structure of Apricot pectin polysaccharides is discussed from both literature and recent work we have performed. Structural characterization utilized 1D and 2D homo- and hetero-nuclear NMR spectroscopy including results from High Performance Size Exclusion Chromatography (HP-SEC), HP Anion-Exchange Chromatography with Pulsed Amperometric Detection (HPAEC-PAD) and FTIR spectroscopy. The purified pectin fraction (F1AP) was found to be composed of D-galacturonic acid, L-rhamnose, D-arabinose and D-galactose in a 1.0 : 0.1 : 0.36 : 0.12 molar ratio, respectively, which is consistent with a pectin RG-1 branched with arabinogalactan side chain polysaccharides, and has a weight-average molecular weight of approximately 1588.2 kDa. The slope of the hydrodynamic radius versus the molar mass was 0.57, indicating the presence of coil conformations. The results from HPAEC-PAD, HPSEC and NMR spectroscopy (^{1}H, ^{13}C, zTOCSY, HSQC, HSQCTOXY and HMBC) demonstrated that F1AP fine fraction F1AP1, derived from original F1AP, has a backbone of (1→4)-linked -D-galacturonic acid and -L-rhamnopyranosyl residues branched with arabinogalactan of multiply glycosidic linkages of T- α-Araf, 3-α-Araf, 5-α-Araf, T- α -Arap, 2- α-Arap side chains, having methyl and acetylated groups, and has high molecular weights (1945 kDa). While the other F1A6 fraction consists predominately of an HG region of pectin polysaccharides with low molecular weights (117.5 kDa), less aggregated. The F1AP1 polysaccharide was highly viscous and its hydrodynamic radius was 64,3 nm. The exponent b of Rh-Mw (conformation plot) was determined to be 0.48, indicating a compact flexible coil conformation of the macromolecule in solution. However, the F1AP6 fraction of apricot fruits belong to backbone of repeats units of [-(1→4)-α-D-GalpA-1]n – both HG and partly contents RG-II polysaccharides, bearing heterosugar sidechains, including α-Ara, α -Rha and β-Gal residues and adopt more stiffness rod like conformation.

Keywords: apricot pectin; NMR spectroscopy; RG-I; HG; RG-II; arabinogalactan; molecular weight; conformation

1. Introduction

Apricot (*Prunus armeniaca L.*) fruits are widely consumed in the world, and their growth is widespread throughout Central Asia, both in the wild and in cultivation. *Prunus armeniaca* is the most commonly cultivated apricot species. The native range is somewhat uncertain due to its extensive prehistoric cultivation. Genetic studies indicate Central Asia is the center of origin [1]. It is extensively cultivated in many countries and has escaped into the wild in many places [2]. Apricots have been cultivated in Persia since antiquity, and dried ones were an important commodity on Persian trade routes. Its introduction to Europe is attributed to Alexander the Great [3]. Apricots remain an important fruit in Tajikistan.

There are more than 60 varieties of apricot, and they are consumed immature, mature, and in dried forms. Common preparations include jams, jellies, canned fruits, bakery fillings, and compotes.

Preprints (www.preprints.org) | NOT PEER-REVIEWED | Posted: 4 December 2023 doi:10.20944/preprints202312.0151.v1

In addition, traditional medicines have long used all parts of the plant for therapeutic purposes. The fruit contains high levels of dietary fibers, minerals, vitamins, and carotenoids and can be considered a very rich source of bioactive phenolic compounds, including catechins, phenylpropanoid (chlorogenic, gallic, ferulic, caffeic, 4-aminobenzoic, pyrocatechinic, salicylic, and p-coumaric) acids, procyanidins, and phenolic glycosides [3–8]. The major flavanols includes quercetin, glycoside rutin, resveratrol, and vanillin [3], which contribute significantly to their taste, color and nutritive value [5]. These fruits are also containing carotenoids such as carotene, β-carotene, lycopene, cryptoxanthin, phytoene, phytofluene, and lutein [4–8].

The nutrient composition of fruits and vegetables is complex and challenging to assess. Apart from its phytochemicals, the pharmacological significance of this fruit is due to having high amounts of high molecular weight (polysaccharides) including pectin and low molecular weight carbohydrates (oligosaccharides) [6–9].

Pectin is one of the major plant cell wall components and the most complex macromolecule in nature, as it can be composed out of as many as 17 different monosaccharides containing more than 20 different linkages, the structural variation in pectin's depending from different developmental stages or from different sources [10–12]. The pectic polysaccharides have a complex structure but can generally be divided into homogalacturonan (HG), rhamnogalacturonan-I (RG-I), rhamnogalacturonan II (RG-II) and xylogalacturonan (XGA). These polysaccharides appear to be present in all cells but their relative abundance and structural details differ between cell types and species [11,12]. RG-I has a backbone of -4)-α-D-GalpA-(1 → 2)-α-LRhap-(1- and side branches composed mainly of neutral sugars (NS), arabinan and galactan motifs, and are of highly variable structure and composition.

The manner with which these polymers are attached or become entangled with each other and cellulosic polymers to form the pectin matrix has been a matter of debate. The classical theory is that the RG-I and HG polymers alternate with each other as block polymers and that the side chains interact with neighboring polysaccharide chains. Recently, this standard theory has been questioned and an argument whereby the HG polymers are actually side chains of a RG-I backbone polymer has been advanced [10].

The pectin matrix is now believed to contain sub-domains of RG-I, HG and RG-II which may interact with different polysaccharide components of the cell wall such as cellulose or xyloglucan [11] (Figure 1). Several lines of evidence suggest that galactan-rich forms of RG-I contribute to the firmness of multicellular plant tissues, while arabinans have been associated with elasticity in guard cells [13]. Additionally, arabinan- and galactan-rich side chains have high mobility and likely water-holding properties [13–15].

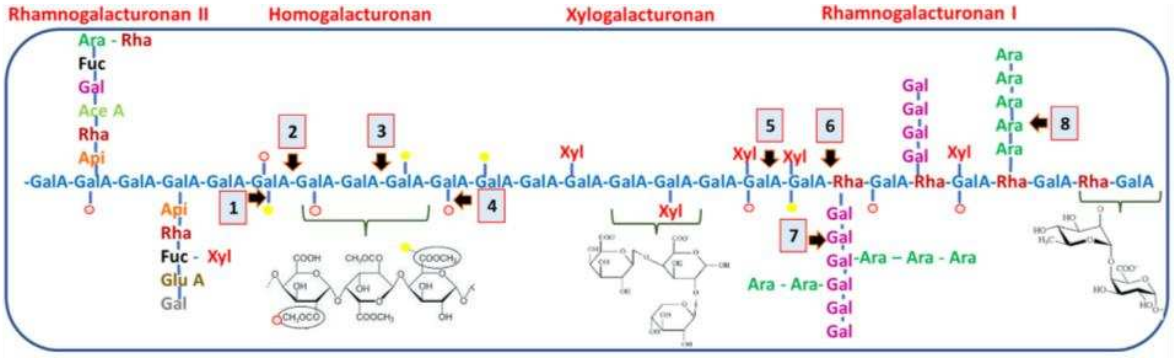

Figure 1. Structure of four pectic polysaccharides, homogalacturonan (HG), xylogalacturonan (XGA), rhamnogalacturonan I (RG-I), and rhamnogalacturonan II (RG-II), linked to each other that are found in Arabidopsis plants (Scheller et al., 2007 [11]).

RG-II is structurally unrelated to RG-I and is an HG backbone consisting of approximately nine 1,4-linked α-D-GalA residues that may be methylated at the C-6 position [16].

Pectin shows multifunctional applications including in the food industry, the health and pharmaceutical sector, and in packaging regimes. Pectin is commonly utilized in the food industry

 doi:10.20944/preprints202312.0151.v1

as an additive in foods such as jams, jellies, low calorie foods, stabilizing acidified milk products, thickener and emulsifier. Pectin is widely used in the pharmaceutical industry for the preparation of medicines that reduce blood cholesterol level and cure gastrointestinal disorders, as well as in cancer treatment. Pectin also finds use in numerous other industries, such as in the preparation of edible films and coatings, paper substitutes and foams. The multifunctionality of pectin is related to the nature of its molecule that has diverse chemical structures, physicochemical properties and potential functionalities depending on the sources where it is extracted and on the extraction methods [17].

Due to these varied uses of pectin in different applications, there is a great necessity to explore other non-conventional sources [18]. The pectin content for non-conventional sources including fruits and vegetables such as apricot, cherries, orange and carrots are 1%, 0.4%, 0.5–3.5% and 1.4%, respectively, on a fresh weight basis [19]. The biological active compounds of Apricots fruits have potent antioxidant activity and is proven to provide important health benefits such as reducing oxidative stress, boosting the immune system, decreasing the risk of heart disease, inflammation, arthritis, and some forms of cancer, and protecting against age-related macular degeneration [3–9,18–22]. Under rigorously controlled experimental conditions, fruit and vegetable consumption, especially apricot fruits are associated with a decrease in blood pressure, which is an important cardiovascular risk factor. However, the effects of fruit and vegetable consumption on plasma lipid levels, diabetes, and body weight have not yet been thoroughly explored [20]. The anti-diabetic activities of apricot fruits, α-glucosidase inhibitory activity, and antioxidant activity of neutral polysaccharides from apricot have gained significant interest among recent publications [20–23].

We previously reported the effect of pectin from different fruit sources (apricot, peach and quince pectin) on the biosynthesis bile acids and cholesterol levels in rats [20]. Concomitant examination of bile flow and the biliary secretion of the lipids were significantly different between animals receiving a crude pectin-supplemented diet, which contained pectin oligosaccharides and polyphenols. In rats fed pectin, biliary cholesterol and bilirubin levels were significantly lower, but the phospholipids and bile acid pool sizes were significantly greater than in the control group. Similar changes of greater magnitude were found in rats fed peach and apricot pectin, but lower magnitudes were found in rats fed quince pectin. With repeated administration of peach pectin, bile secretion, compared with the control, increased by 48%, and quince pectin - by 60%. A great effect was observed with apricot pectin, with its repeated administration [20].

Identification and quantification of the poly- and oligosaccharides in fruits and vegetables is a challenging area as these foods contain a complex mixture of carbohydrates with a varying chain length from 2 to 2500 units. However, according to our knowledge, this is the ever first study carried out on the composition and structures of pectin polysaccharides from apricots fruits using NMR spectroscopy methods.

NMR is an important spectroscopic technique for analyzing biomolecules to characterize their physical characteristics and determine their structures [24,25]. Owing to their large sizes and complex, branched structures, often with repeating, or nearly-repeating sequences, carbohydrates in general, and specifically pectin, have unique challenges when analyzed by NMR. Yet, useful information can nonetheless be acquired. The fine structure of pectin polysaccharides will be discussed in this article from both literature and recent work we have performed on apricot pectin [24–27].

2. Results

2.1. Isolation and Purification of pectin Polysaccharides

Apricot fruits “Mahtobi” (Figure 2.) grown in Tajikistan were purchased in May month

Preprints (www.preprints.org) | NOT PEER-REVIEWED | Posted: 4 December 2023 doi:10.20944/preprints202312.0151.v1

Figure 2. Apricot specie "Mahtobi" growing in Tajikistan.

From fruits weighing 4450 were separated kernel (630 gr) and squeezed the juice (1800 mL). The residual mass of wet and dry mass of apricot fruit pomace accounted for 1750 and 250 grams respectively (Figure 3). A hydrolysate solution from the rest of the cell was separated by filtration, then cooled with ice containers and neutralized to pH 3.4. The supernatant solution (fraction F1) and residual precipitate, microgel (F2) were separated by centrifuge.

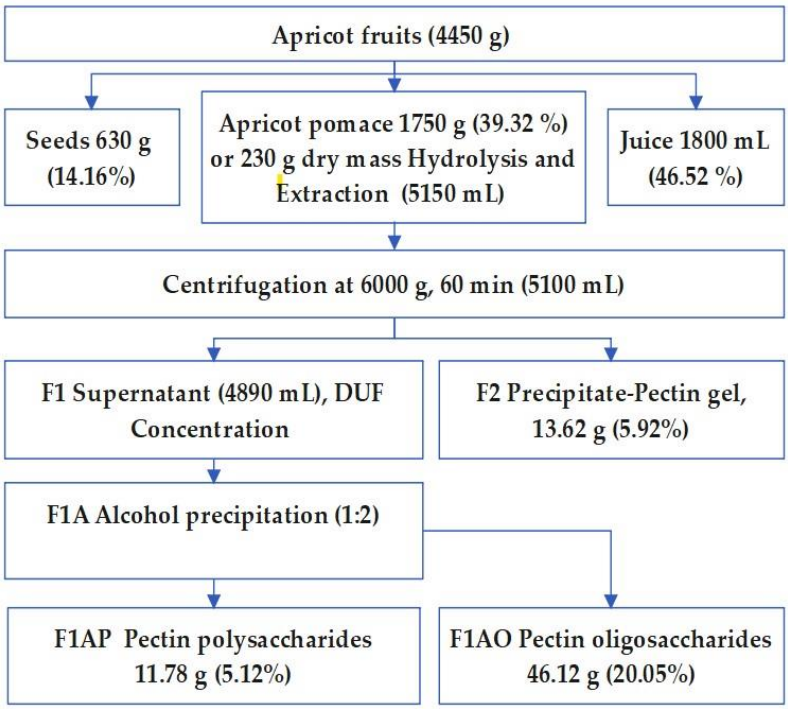

Figure 3. Extraction scheme of pectin poly- (F1AP) and oligosaccharides (F1AO) fraction from Apricot fruits.

Thus, a purified hydrolysate solution forced to the diaultrafiltration (DUF) via 100 KD PS membrane using the DUF systems (KrosFlo, USA) to separate and concentrate pectin polysaccharides, which further was extracted by alcohol precipitation (fraction F1AP), accounted for 5.12% of apricot dry mass. An alcoholic soluble fraction was concentrated on a rotary evaporator to obtain oligosaccharide and polyphenol (F1AO) (Figure 3).

Permeate of PS 100KD (1500 ml) was undergo subsequent membrane filtration using two types of membrane: 5KD and 1Kd molar amass cut off (MCO) types respectively. The received concentrated solution of 5KD MCO further referred as F1B1 and it permeate as F1B2 consequently, the results not discussed in this work.

The deprotonated pectin polysaccharide has been further fractionated by anion-exchange chromatography as described early [27]. Further refinement of the polysaccharides proceeded by loading on anion-exchange column of a DEAE Sepharose. The elution profile of the F1AP sample (tubes 1-34) with deionized water (Figure 4) indicates that the main fraction of the apricot polysaccharide, having low negative charge, eluted from tubes 10 to 18 by water. The main polysaccharide components of apricot pectin eluted by water, which accounted for 67.14% of the

Preprints (www.preprints.org) | NOT PEER-REVIEWED | Posted: 4 December 2023 doi:10.20944/preprints202312.0151.v1

F1AP, further named as F1AP1 fraction. It also shows the profile of the several fractions of polysaccharides, eluted from the DEAE Sepharose anion-exchange column by NaCl solutions of increasing ionic strength (0.01, 0.03, 0.05, 0.07, 0.2, 0.3, and 0.5) at a flow rate of 5 mL/min (Figure 4). The next major polysaccharide components of apricot pectin polysaccharides eluted by 0.2 M NaCl, accounted for 22.85% and referred as F1AP6. This indicate that F1AP6 fraction has high negative charge that were retained on anion-exchange column.

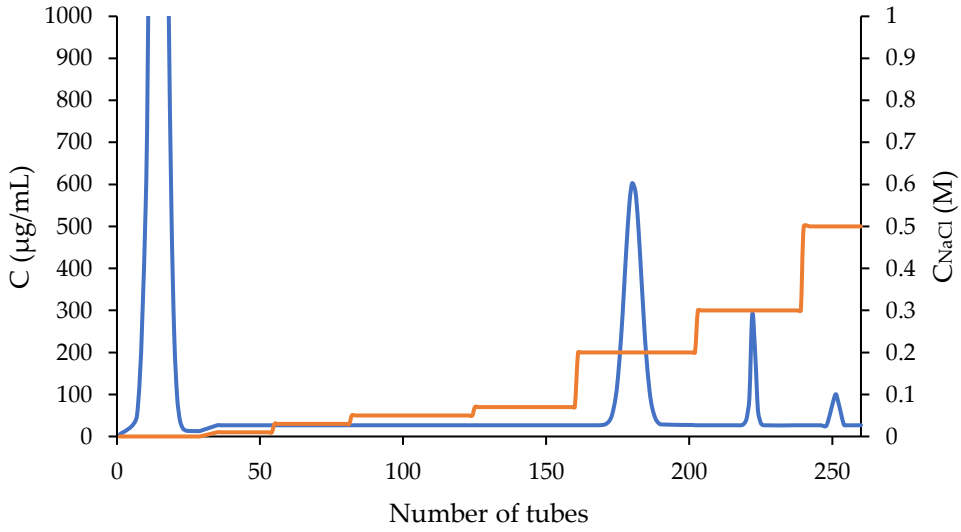

Figure 4. Elution profile of the Apricot pectin polysaccharides from DEAE Sepharose anion-exchange column (blue line). Gradient of NaCl ionic strength (0, 0.01, 0.03, 0.05, 0.07, 0.2, 0.3, and 0.5 M) at a flow rate of 5 mL/min (red line).

Other five minor fractions with different charge density were eluted from the F1AP sample by the rising concentration of NaCl solutions of 0.01 M (tubes 35–54), 0.03 M (tubes 55–81), 0.05 M (tubes 82–124), 0.07 M (tubes 125–160), 0.2 M (tubes 161-202), 0.3 M (tubes 203-239), and 0.5 M (tubes 240-260). The remaining fractions were too small for extensive structural analysis.

2.2. Monosaccharide composition of Apricot pectin (F1AP), its main fractions F1AP1, F1AP6 and pectin oligosaccharides (F1AO)

The monosaccharide compositions of the original and two main fractions were analyzed by HPAEC-PAD. The original fraction (F1AP) composed of D-galacturonic acid, L-rhamnose, D-arabinose and D-galactose in a 1.0 : 0.1 : 0.36 : 0.12 molar ratio, respectively, which is consistent with a pectin RG-1 branched with arabinogalactan side chine poly-saccharides. The water-eluted fraction F1AP1 was found to have almost the same composition reviled to branched RG-1, while bounded on DEAE Sepharose anion-exchange polysaccharide might belong to the HG reigns of pectin polysaccharides. The alcohol soluble fraction comprises 93.26 % D-glucose with some impurities of related monosaccharides, mostly of arabinose and xylose trace.

Table 1. Monosaccharide composition (%) of the apricot F1AP, F1AP1 and F1AP6.

Apricot pectin	Glc	Man	Ara	Gal	Xyl	Rha	Fuc	GalA	GlcA
F1AP	2.93	0	21.3	6.83	2.32	5.4	0.4	59.7	1.1
F1AP1	0.98	0	25.8	5.61	1.60	6.9	0.4	58.1	0.8
F1AP6	0.13	0	8.47	3.66	0.50	2.1	0.2	83.9	1.0
F1AO	93.26	0.94	2.95	0.58	1.25	0.31	0.03	0.36	0.33

Preprints (www.preprints.org) | NOT PEER-REVIEWED | Posted: 4 December 2023 doi:10.20944/preprints202312.0151.v1

As seen from this table, Ara, Gal, and Rha were dominant sugars in the apricot pectin, while other monosaccharides like xylose, glucose, and fucose were present in minor amounts. The higher amount of arabinose is peculiar to the apricot pectin. However, this pectin, compared to other studied apricot species [28], is distinguished on mannose quantity. This pectin has no or very minor quantity of Man. It is visible that after fractionation, moving from the original F1AP to the fraction eluted by water from DEAE anion exchange columns F1AP1, the content of Ara and Rha increased. The fraction linked to the DEAE, eluted by 0.2M NaCl, exhibited a higher content of GalA (83.9%) residue with a reduced quantity of neutral sugars. From monosaccharide composition analysis, the F1AP1 attributed to the RG-1 pectin, bearing arabinogalactan side chain. In other hand the fraction eluted by 0.2 M, NaCl dominated by the HG regions of pectin polysaccharides.

The study of the cell wall matrix polysaccharides contents using sequential solubilization and antibody-based approaches in association with anion-exchange chromatography analysis indicates that in all cases, solubilized polymers include spectra of HG molecules with unesterified regions that are separable from methyl esterified HG domains [15]. In highly soluble fractions, RG-I domains exist in both HG-associated and non HG-associated forms.

We can preliminarily conclude that the studied pectin fraction F1AP1 is mainly composed of L-Ara and D-Gal, L-Rha, and D-GalA, as expected, forming a water-soluble complex of RG-I with an arabinogalactan side chain. Another fraction, F1AP6, contains highly charged HG residues, likely RG-II residues with AG side chains that represent the pectic polysaccharides in the cell wall of Apricot fruits.

2.3. Analysis of ATR-FTIR spectra of Apricot pectin polysaccharides

Apricot pectin polysaccharide samples, in the form of dry powder, were stored in P_2O atmosphere before analysis. ATR-FTIR spectra data (4000 to 600 cm^{-1}) were acquired at room temperature in a NicoletTM iSTM 50 FTIR (Thermo Fisher Scientific).

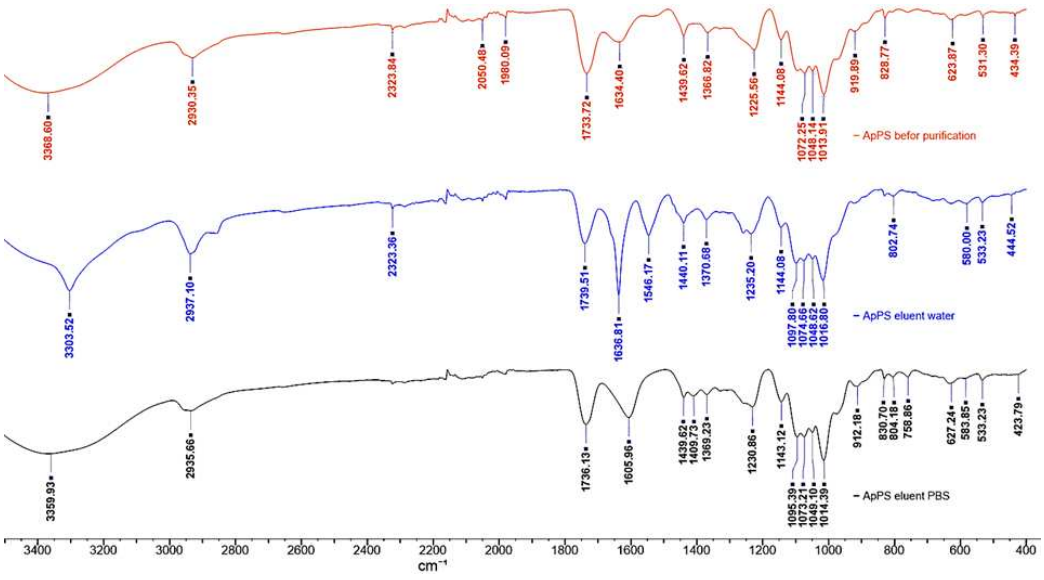

Figure 5. Comparison of ATR-FTIR spectra of Apricot pectin polysaccharides: F1AP (red); F1AP1 (blue) and F1AP6 (black) in regions of 4000-400 cm^{-1}.

Relevant wavenumbers were highlighted for each pectin samples (Figure 5): The 4000 to 2100 cm^{-1} spectral region is dominated by the broad and intense O-H stretching band of hydroxyl groups, overlapped with the C-H stretching bands. The broad shoulder near 2550 cm^{-1}, observed only in water eluted F1AP1 fraction may be assigned to the O-H stretching vibration in free carboxyl groups [29]. The two strong bands in the 1750-1500 cm^{-1} region are assigned to stretching vibration modes of carbonyl groups from esterified D-GalA units and free carboxylate groups, respectively [30]. Herewith, absorbance at the 1733-1739 cm^{-1} attributed to the ν(C=O) esterified and that at the 1605-

 doi:10.20944/preprints202312.0151.v1

1636 cm^{-1} belong to free acid and ionized carboxyl group of pectin fractions according to the D-GalA unit environments and its degree of methylation.

The main CHx and C-O-H deformation modes appear partially overlapped, in the 1500-1200 cm^{-1} region The characteristic bending asymmetric vibration of δas(CH_3) methyl group appears in the region of 1439 cm^{-1} and symmetric vibration of δs(CH_3) acetyl grout in the region of 1366-1370 cm^{-1} . The new weak peak at the 1409 cm^{-1} of F1AP6 in combination of peeks at the 1231 and 1073 can be assigned to presence of RG-1 [31].

The absorption bands in fingerprinted region, overlapped bands observed in the 1200-950 cm^{-1} characteristics for stretching asymmetric vibration of pyranose C-O-C and are characteristic of the pectin backbone and side groups. The band at 1144 cm^{-1} is assigned to the C-O-C stretching vibrations of the α-1,4-D-glycosidic bonds in the HG chains. The strong bands at 1014 cm^{-1} in IR spectra of the of original F1AP and F1AP6 are due to skeletal stretching modes of the pyranose rings in D-GalA and L-Rha residues, present both in HG and RG regions. In case of F1AP1 fraction was moved to upper filed at 1018 cm^{-1} due to predominance of HG region in this fraction. The other two parallel bands, at 1072 and 1048 cm^{-1}, in the original pectin occur at 1097 and 1074 cm^{-1} in the IR spectra of F1AP1 and F1AP 6 fractions, result from neutral sugars in the side chains of RG-I and are assigned to the same stretching modes of L-arabinosyl and D-galactosyl units, respectively [31–34]. In aqueous solutions, Kacurakova et al. (2000) observed bands at 1070 and 1043 cm^{-1} for rhamnogalacturonan, 1072 cm^{-1} for galactan and 1039 cm^{-1} arabinan, which were too close for reliable discrimination [35]. These differences may be due to the different states (solid or solution) of the cell wall compounds and probably also to the specificity of the used spectrometers. For pectic homogalacturonans with more or less methylation, the main characteristic peaks (especially 1740, 1600, 1097 and 1014 cm^{-1}) were stable regardless of whether they are in a solid crystalline state or in an aqueous solution [31].

Some band positions were affected by macromolecular arrangements. In fact, the key monosaccharides, galactose (Gal) and arabinose (Ara), were shown to have intense peaks at about 1074 and 1048 cm^{-1}. The variable region was identified to be at about 1134-1094 cm^{-1} and 900-819 cm^{-1} and was probably due to compositional and structural differences between pectin polysaccharides fractions.

We ought to note that apricot pectin entails a complex group of heteropolysaccharides containing different covalently interlinked pectic polysaccharide types, of which HG, RG-I, and, to a lesser extent, type II rhamnogalacturonan (RG-II) and xylogalacturonan (XGA) are the most common. Therefore, the application of ATR-FTIR could sometimes remain limited for linkage structural elucidations due to the complexity of overlapping spectra bands and vibrational coupling from the enormous diversity of CWP chemical bonds.

From IR spectra it is possible to evaluate the degree of esterification of carboxyl group of pectin fractions. The degree of esterification of pectin (percent of methyl-esterified carboxyl groups) was determined by the using an approach provided by calculated simply by using the intensity of the asymmetric stretching of CH_3 at 1440 cm^{-1} relative to a backbone vibration at 1010 cm^{-1} [36].

DE (F1AP) = 455*(A_{1440}/ A_{1016}) +2 =455*(0,10/0,69)+2=66.5%
DE (F1AP1) = 455*(A_{1439}/ A_{1014}) +2 =455*(0,11/0,69)+2=74.5%
DE (F1AP6) = 455*(A_{1441}/ A_{1013}) +2 =455*(0,09/0,87)+2=49.0%

From these results it is clear that solubilization of F1AP1 fraction influenced by DE of pectin. However, additional information would be needed to determine the exact reason for this variation.

Preprints (www.preprints.org) | NOT PEER-REVIEWED | Posted: 4 December 2023 doi:10.20944/preprints202312.0151.v1

2.4. Analysis of molar mass and molar mass distributions (MMD) of Apricot pectin polysaccharides by size exclusion chromatography (SEC)

The pectin molar mass and molar mass distribution (MMD) were measured by high-performance size exclusion chromatography (HPSEC) using multi-detection systems. (Materials and Methods, section 3.2). The brief molar mass and MMD analyzes of main Apricot pectin and its fine fraction, as described previously with the aid of HPSEC by MALLS [27], are provide in this work. The F1AP LS chromatogram main peak 1, eluted at 12.3-16.6 mL and represented 77.5% of the molar weight (Figure 6). The LS of MALLS shows non symmetric peak, a bimodal distribution at least of two fractions in the Apricot pectin.

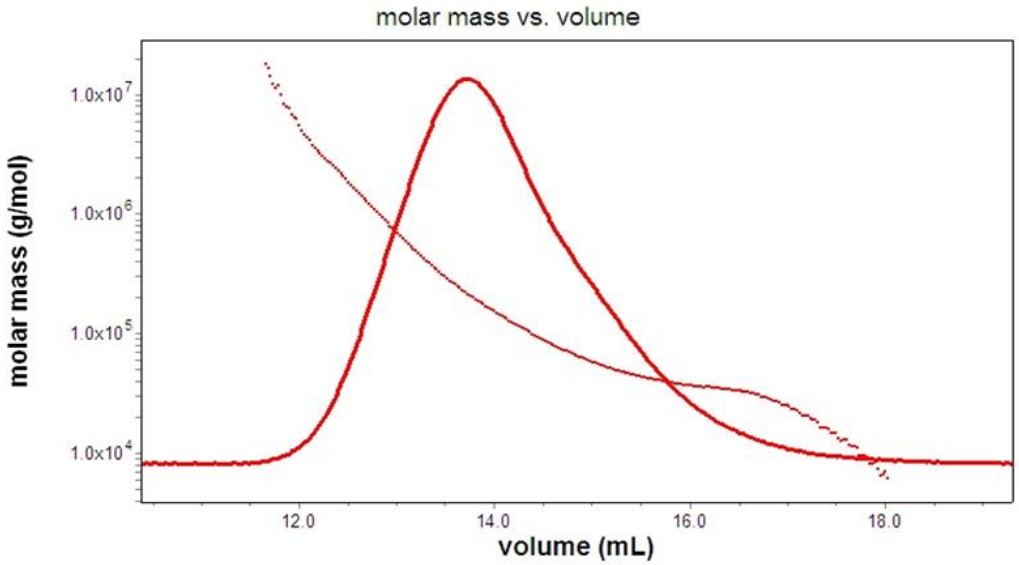

Figure 6. HPSEC chromatograms from LS detector of F1AP and molar mass distribution curve.

The shapes and forms of the macromolecules were assessed based on their measured molar masses and their hydrodynamic radii, as obtained from their intrinsic viscosity. The dependence of molar mass and hydrodynamic radius (R_h conformation plot) were analyzed by the ASTRA software (V.7.1.2.5, Wyatt Technology). The slope of this graph allows one to estimate the shape of a homogeneous polymer [26,27]. In the case of a heterogeneous polymer, the relationship between the slope and the molecular shape is somewhat more complicated as indicated in Figure 7 for a F1AP sample.

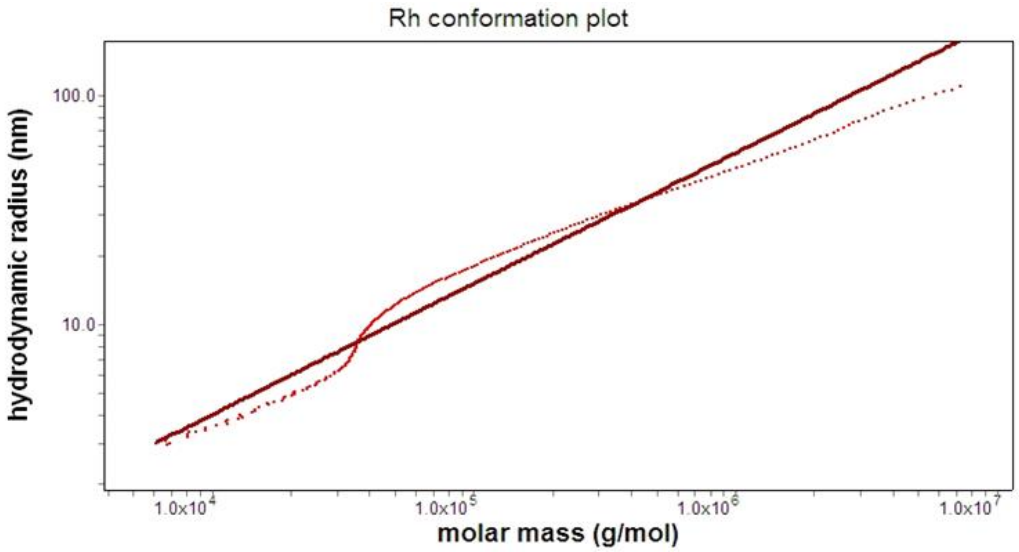

Preprints (www.preprints.org) | NOT PEER-REVIEWED | Posted: 4 December 2023 doi:10.20944/preprints202312.0151.v1

Figure 7. Hydrodynamic radius versus the molar mass (R_h conformation plot) of the F1AP. The slope value is 0.57.

Table 2 displays the results of the measurements of the polydispersity (M_w/M_n, M_z/M_n), number average molar mass (Mn), weight average molar mass (M_w), z-average molar mass (M_z), intrinsic viscosity [η_w], hydrodynamic radius [R_h], from each sample. A distinct bimodal peak is observed in the DV and IR chromatograms of original F1AP pectin, as compared to F1AP1 and F1AP6 fractions. The F1AP1 versus F1AP6 data analyzed as a single peak for the total chromatograms had following M_w, η_w, R_h values, 1945:117 kDa, 426:158 mL/mg and 64.3:30.0 nm, respectively.

Pectin oligosaccharides fraction had lower molar mass (3.55 kDa) low viscosity (1.6 mL/mg) and relatively low polydispersity (1.85).

Table 2. Molecular mass and hydrodynamic properties of pectin polysaccharides from apricot fruits.

	R (%)	M_w/M_n	M_w (kD)	✾w, (mL/mg)	R_h (Å)	*b* (R_h conformation plot)
F1AP	77.5	1.92	1588.2	355.1	60.1	0.57
F1AP1	74.3	1.91	1945.0	426.4	64.3	0.48
F1AP6	95.7	2.34	117.5	158.6	30.0	0.78
F1AO	97.1	1.85	3.55	22.0	1.6	-

***Notes**: Percentage of sample recovery (R,%), polydispersity (M_w/M_n), weight average molar mass (M_w), intrinsic viscosity (η_w), hydrodynamic radius (R_h) and **b** value of conformation plot (b).*

The value of η_w, R_h of F1AP6 lower in two time than those of F1AP1 indicating different conformation of pectin fractions. This is consistent with pectin's macromolecule monomer compositions.

Estimated low value of stiffness (flexibility) coefficient 0.57 and 0.48 shows compact flexible coil and random coil conformation for original Apricot pectin and its water-soluble fraction (F1AP1). This analysis indicates the presence of more extend conformations in polysaccharides fraction extracted from DEAE cellulose anion exchange resin by salt solution. The difference in the slope of F1AP1 vs F1AP6 indicates its structure diversity, as follows from its monosaccharide composition. At the same time, F1AP6 has more homogeneity in structure rod-like molecular shapes (b=0.78), which agrees with the high content of galacturonic acid residues (GalA) in this fraction (Table 1). The chain stiffness of the original Apricot pectin and its F1AP1 fraction, except F1AP6 fraction, have similar conformations to those found previously for studied pectin poly-saccharides from different origin dominance with RG regions [26,37]. The conformation of F1AP6 fraction is close to that of sunflower pectin, which contains high HG regions.

A combination analysis of pectin conformations together with pectin GalA content (Table 1) and its DE in RG-I backbone studied by other authors [38,39] indicate that, the elevated degree of GalA esterification in the high-molar mass fraction (F1AP1) would be expected to reduce calcium cross-linking, thus hindering the formation of an open, well-spaced pectin network in the solution. Alternatively, the lower negative charge of GalA region might increase intermolecular interactions between HG chains or between HG and RG-I or RG-II thus facilitating aggregation. The high degrees of methylesterification of the polysaccharide promote intermolecular hydrophobic interactions.

2.2. Carbohydrate Methylation Analysis of the Apricot pectin

The methylation analysis was demonstrated only for original purified apricot pectin, F1AP sample in according with methods detailed by Heiss et al., 2009 [40]. Relative percentage of each detected linkage in F1AP sample, generated from Total Ion Chromatogram of the partially methylated alditol acetates (PMAA) derivatives (Figure S1). The results of the major glycosyl linkage

 doi:10.20944/preprints202312.0151.v1

compositions are presented in Table 3. From this Table, it is clear that the main polysaccharide backbone of apricot pectin was comprised of 4-, 3-, and terminal (t) linked Galactopyranosyl uronic acid residues (GalpA, 69.04 %); 2-, 2,3- 2,4- linked Rhamnopyranosyl residues (Rhap, 6.19%,); t-, 2-, 3-, 5- linked Arabinofuranosil (Araf, 5.32%); t-, and 3- linked Arabinopyranosyl residues (Arap, 4.72%); t-, 2-, 3-, 4-, 6-, 3,6-, 4,6- linked Galactopyranosyl residue (Galp, 9,17%). These sugar residues almost accounted for 94,44 % of PMAA from hydrolysate of pectin polysaccharides in Apricot pectin.

Table 3. Relative percentage of each detected linkage in F1AP sample, generated from Total Ion Chromatogram feature in Data Analysis. The TIC peaks are given in order to increasing retention time.

Linkage patterns	Relative area percentage (%)
Terminal Rhamnopyranosyl residue (t-Rha)	0.52
Terminal Arabinofuranosyl residue (t-Araf)	3.80
Terminal Arabinopyranosyl residue (t-Ara)	4.60
Terminal Xylopyranosyl residue (t-Xyl)	0.58
2 linked Rhamnopyranosyl residue (2-Rha)	4.67
2 linked Arabinofuranosyl residue (2-Araf)	0.25
Terminal Glucopyranosyl residue (t-Glc)	1.69
3 linked Arabinofuranosyl residue (3-Araf)	0.42
Terminal Galactofuranosyl residue (t-Galf)*	0.32
Terminal Galactofuranosyl uronic acid residue (t-GalA)*	0.33
Terminal Galactopyranosyl residue (t-Gal)	3.70
Terminal Galactopyranosyl uronic acid residue (t-GalA)	3.32
5 linked Arabinofuranosyl residue (5-Araf)	0.85
3 linked Arabinopyranosyl residue (3-Ara)	0.12
2 linked Xylopyranosyl residue (2-Xyl)	0.17
4 linked Xylopyranosyl residue (4-Xyl)	0.26
2,3 linked Rhamnopyranosyl residue (2,3-Rha)	0.20
2,4 linked Rhamnopyranosyl residue (2,4-Rha)	0.80
3 linked Galactopyranosyl residue (3-Gal)	1.39
2 linked Galactopyranosyl residue (2-Gal)	0.12
4 linked Galactopyranosyl residue (4-Gal)	1.41
4 linked Galactopyranosyl uronic acid residue (4-GalA)	62.2
4 linked Glucopyranosyl residue (4-Glc)	2.12
4 linked Glucopyranosyl uronic acid residue (4-GlcA)	0.37
6 linked Galactopyranosyl residue (6-Gal)	1.81
3,4 linked Galactopyranosyl residue (3,4-Gal)	0.10
3,4 linked Galactopyranosyl uronic acid residue (3,4-GalA)	1.83
2,4 linked Galactopyranosyl residue (2,4-Gal)	0.07
2,4 linked Galactopyranosyl uronic acid residue (2,4-GalA)	0.67

Preprints (www.preprints.org) | NOT PEER-REVIEWED | Posted: 4 December 2023 doi:10.20944/preprints202312.0151.v1

4,6 linked Glucopyranosyl residue (4,6-Glc)	0.73
4,6 linked Galactopyranosyl residue (4,6-Gal)	0.04
3,6 linked Galactopyranosyl residue (3,6-Gal)	0.63

**The terminal galactofuranosyl residue and its respective uronic acid residue are probably artifacts of the procedure. During methanolysis, the pyranosyl ring can open and then close as a furanosyl. In the raw data, the 4-GalA corresponding with the 4,6-Gal eluting before 22 min is labeled as 4,6-GalA. A 6 linked uronic acid structure is from the method when there is undermethylation of that 6 position. For accuracy in the report, the 4,6-GalA residue area has been added to the 4-GalA residue, but it remains separate in the raw data. Mass spectra for each identified peak are included in the raw data file.*

The rest monosaccharide residues reflected trace amounts the 4- and 4,6- linked Glucopyranosyl residue (Clcp, 4.23%), and t-, 2- and 4-linked xylopyranosyl (1,01%), which were indicative of Xylogalacturonan fragments resulted from hemicellulose by flash hydrolysis. The existence of t-Clcp residues (1.69%) because of starch or endosperm sugars.

A different linkage proportion of Arap, Araf and Galp residues was postulated as highly branched arabinan and galactan short side chains. This three-type side chain should be attached to the backbone of RG-I at C(O)3 and C(O)4 positions because of the presence of 2,3- and 2,4-linked Rhap residues resulted from methylation analysis.

The number of terminal Araf, Rhap and Clcp residues was approximately equal to the number of branched residues, suggesting that the methylation process used was effective. Besides, it indicated a correlation between terminal and branched residues. The backbone and branch of original F1AP pectin contained multiple linkage types and the most common derivatives were consistent with the monosaccharide composition identified via HPAE-PAD method.

3.1. NMR Spectroscopy

3.1.1. NMR analysis of original Apricot pectin (F1AP sample)

^{1}H and ^{13}C NMR spectra of Apricot pectin polysaccharides are presented in the Figure S2 of supplementary materials: (a) F1AP; (b) F1AP1; (c) F1AP6.

The 2D-HSQC spectrum was acquired both at 45 °C and 80 °C. Figure 8 demonstrated 2D-HSQC spectrum at 80 °C, where four anomeric peaks are observed.

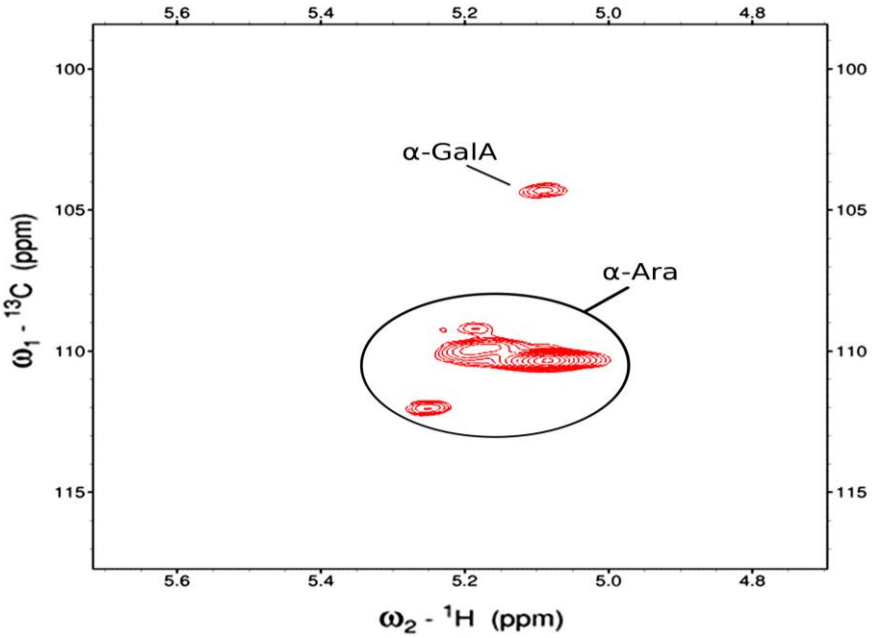

Figure 8. The anomeric region of F1AP1 is shown in the HSQC spectrum at 80°C.

Preprints (www.preprints.org) | NOT PEER-REVIEWED | Posted: 4 December 2023 doi:10.20944/preprints202312.0151.v1

These peaks have proton resonances that are typical for sugars with H1 and H2 in an axial–equatorial orientation, or α conformation. The three peaks observed at ~110 ppm in the ^{13}C dimension were readily assigned as α-Ara based on their distinctive resonances. A weaker anomeric peak is at 5.01/104.3 ppm ($^{1}H/^{13}C$) is likely to be α-GalA, based on comparisons of literature chemical shift values and the monosaccharide analysis. These anomeric resonances are common to fractions F1AP1 and F1AP6 as well. In addition, a methyl resonance was found at 1.254/19.39 ppm which is consistent with H6/C6 of an α-Rha. In the other fractions of this sample, a COSY cross peak is observed connecting it to the H5. The spectra also indicate the presence of a methyl ester group (3.811/55.62 ppm), two methoxy groups (2.081/22.99 and 2.175/23.22 ppm) and one acetyl methyl (3.351/51.78 ppm), however it was not possible to determine their through-bond connectivity.

The assigned ^{1}H and ^{13}C chemical shifts from the 2D NMR experiments at 45 °C are given in Table 4, and are based on through-bond correlations as well as comparisons to literature values for chemical shifts.

Table 4. Monosaccharide assignments from 2D experiments.

	C1	C2	C3	C4	C5	C6	H1	H2	H3	H4	H5	H6	H (Unassigned)
α -Rha	-	-	-	-	-	19.39	-	-	-	-	-	1.254	
α -Ara	112	86.78	-	-	-	-	5.252	-	3.958	3.717	-	-	4.071, 3.83
α -Ara	110	-	-	-	-	-	5.189	4.213	4.006	-	-	-	
α -Ara	109.8	-	-	-	64.07	-	5.164	4.139	3.973	-	3.734, 3.832	-	
α -Ara	110.3	83.67	79.58	85.14	69.75	-	5.088	4.133	4.018	4.213	3.805, 3.885	-	
α -GalA	104.3	65.87	66.03	65.9			5.091	3.817	3.723	-	4.031	-	-

In addition, a methyl ester group (3.811/55.62 ppm for $^{1}H/^{13}C$), two methoxy groups (2.081/22.99 and 2.175/23.22 ppm) and one acetyl methyl (3.351/51.78 ppm) were also observed.

3.1.2. NMR analysis of F1AP1 fraction of Apricot pectin

This fraction has very high molecular weight of approximately 1945 kDa ($1{,}945 \times 10^{6}$ g/mol), unfavorable t_2 relaxation rates make it difficult to observe anything except the more flexible side-chains of this molecule. Consequently, the 1D-^{1}H spectra consist of a large number of broad and diffuse peaks at both 45 and 80 °C, with the anomeric region being largely uninterpretable. These relaxation properties also result in a 1D-^{13}C spectrum (at 45 °C) with low signal and diffuse peaks. Nevertheless, in the 2D-HSQC spectrum at 45 °C, five anomeric peaks are clearly observed (Figure 9).

All of these peaks have proton resonances that are typical for sugars with H1 and H2 in an axial–equatorial orientation, or α conformation. The four peaks observed at ~110 ppm in the ^{13}C dimension were readily assigned as α-Ara based on their distinctive resonances. A weaker anomeric peak found at 5.1/104.4 ppm (1H/13C) is likely to be α-GalA, based on its resonance frequencies and the concentrations determined by monosaccharide analysis. In addition, one rhamnose was identified by its C6 methyl resonances at 1.25/19.46 ppm ($^{1}H/^{13}C$); it also has a COSY correlation to the H5 at 3.792 ppm (Figure S3).

The heteronuclear HSQC and HSQCTOXY experiments indicate the presence of one methyl ester at 3.82/55.77 ppm (1H/13C), which is presumably attached to a galacturonic acid, although this could not be identified. Also observed are one acetyl methyl (2.100/22.98) and one methoxy (3.36/51.49), each with undetermined attachments.

Preprints (www.preprints.org) | NOT PEER-REVIEWED | Posted: 4 December 2023 doi:10.20944/preprints202312.0151.v1

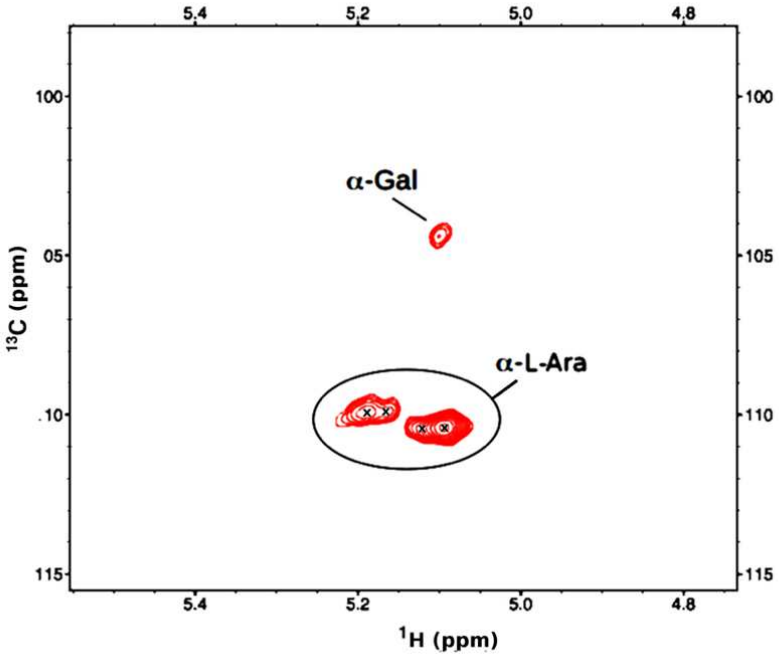

Figure 9. The HSQC anomeric region of the F1AP1 at 45 °C.

In order to improve the relaxation dynamics, the spectra were re-run at 80 °C, resulting in some sharpening of the spectra, the observation of a few more resonances, and some shifting of resonances. The 1D-^{1}H spectrum is still difficult to interpret, but a putative methoxy peak is now observed at ~3.3 ppm. In the anomeric region of the HSQC spectrum the α-Ara peaks are still observed at the same locations but appear to be weaker (Figure 10).

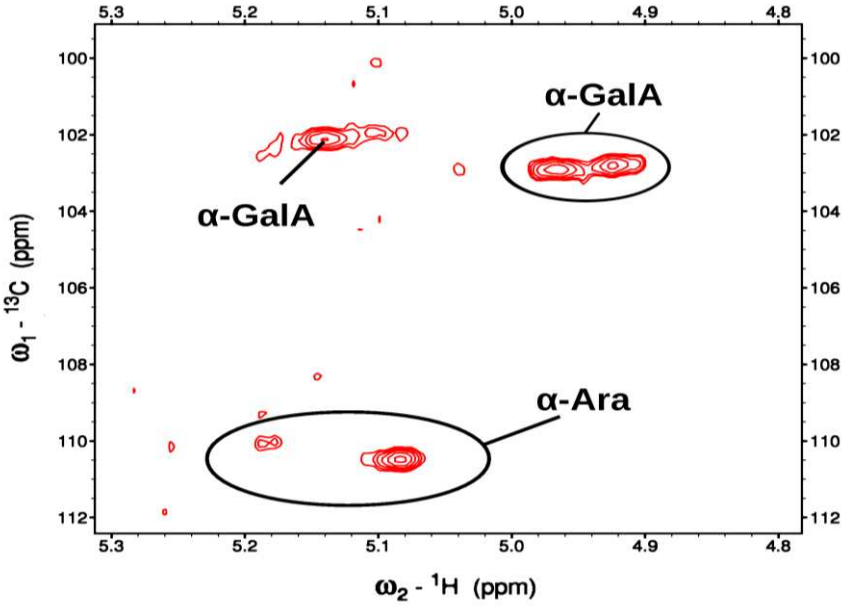

Figure 10. The HSQC anomeric region of F1AP1 sample at 80°C.

It may be that some of the underlying resonances are shifted due to slight variations in the substructure (disaggregation). More notably, there are now at least three α-GalA peaks in the ranges of 4.92-5.14 ppm in 1H and 102.1-102.9 ppm in 13C. These α-GalA are presumably from the main chain, and the overall observations are consistent with previous reports that the rigid backbone of

Preprints (www.preprints.org) | NOT PEER-REVIEWED | Posted: 4 December 2023 doi:10.20944/preprints202312.0151.v1

GalA and Rha produces broad and weak signals. In contrast, the more flexible arabinose side chains result in strong ones [41]. One of these α-GalA was observed in the HMBC to have a methyl ester at 2.82/55.63 ppm (1H/13C). (Table 5).

Table 5. Monosaccharide Assignments of the F1AP1 fraction based on COSY, TOCSY, HSQC, HSQCTOXY and HMBC at 80 °C.

	C1	C2	C3	C4	C5	C6	H1	H2	H3	H4	H5	H6	Hw	Methyl Ester (H/C)
⚜-Rha	-	-	-	-	-	19.46	-	-	-	-	3.792	1.252	-	-
⚜-Ara	110.1	-	-	-	-	-	5.191	-	-	-	-	-	3.788	-
⚜-Ara	110.5	83.9	79.7	85.26	69.84	-	5.086	4.132	4	4.214	3.883, 3.805	-	-	-
⚜-GalA	104.3	66.5	65.97	81.2	74.33	177.7	5.106	3.797	3.727	4.425	4.662	-	-	-
⚜-GalA	102.1	-	-	-	73.32	173.6*	5.133	-	-	-	5.093	-	-	3.821/ 55.63
⚜-GalA	102.9	-	-	-	-	-	4.966	-	-	-	-	-	-	-
⚜-GalA	102.8	-	-	-	-	-	4.924	-	-	-	-	-	-	-
⚜-GalA	99.05						4.589							

** Indicates the methyl-ester attachment.*

A second methyl ester was also observed at 3.84/55.62 ppm, with its carbonyl attachment at 166.0 ppm, but its connection to a sugar could not be determined. As seen at 45 °C, a rhamnose was identified by its C6 methyl resonances at 1.26/19.31 ppm and its COSY correlation to the H5 is at 3.785 ppm. Also, one methoxy group at 3.357/51.89 ppm (H/C), an additional methyl ester at 3.84/55.62 ppm, with its carbonyl attachment at 166.0 ppm, and three acetyl groups: 1.924/25.73 ppm, 2.107/23.15, 2.169.23.38, with carbonyl attachments at 183.2, 176.5 and 176.5 respectively were observed.

The results from HPAEC-PAD, HPSEC and NMR spectroscopy (^{1}H, ^{13}C, zTOCSY, HSQC, HSQCTOXY and HMBC) demonstrated that fraction F1AP1, eluted by water, (accounted for 65.6% of original F1AP pectin) has a backbone of (1→4)-linked -D-galacturonic acid and α-L-rhamnopyranosyl residues branched with arabinogalactan side chains, having methyl and acetylated groups, with high molecular weights (1945 kDa). One of these α-GalA was clearly observed in the HMBC to have a methyl ester at 2.82/55.63 ppm (1H/13C). A second methyl ester was also observed at 3.84/55.62 ppm, with its carbonyl attachment at 166.0 ppm. These α-GalA are presumably from the main chain.

Based on the aforementioned results, we assumed that the main pectin polysaccharides of the F1AP1 fraction in apricot fruits are RG-I polysaccharides (Figure 1, [11]) consisting of the repeating units -[2-α-L-Rha*p*-(1→4)-α-D-Gal*p*A-1]$_n$-. These are substituted with different arabinan sidechains, linked to C(O)4 position of Rha*p* residues. However, galactan and glucan residues were not observed by NMR due to the unfavorable relaxation properties associated with this polysaccharide's very high molar mass and aggregated. The presence of a carbonyl methyl ester in this fraction, identified by FTIR spectra (1740 cm^{-1}) and by ^{1}H/^{13}C NMR (at 2.82/55.63 ppm) indicate that a D-GalA residue in this RG-I pectin is methylated, the DM is 74.5% was found by FTIR.

Carbohydrate analysis and NMR spectroscopy study [11,42] verified that most of the rhamnogalacturonan-I from cultured Arabidopsis cell walls is covalently linked to arabinogalactan-protein complex in cell wall. The study [41] demonstrated that the attached RG-I glycans are decorated with α-1,5-arabinan, β-1,4-galactan, xylose, and 4-O-Me-xylose sidechains, the covalently linked RG-I-AGP is the major component of the traditionally prepared RG-I.

It could be deduced that the acetyl group present in this pectin probably attached to the C(O)2 or C(O)3 position of the GalpA residues. This result was further confirmed by the appearance of a

Preprints (www.preprints.org) | NOT PEER-REVIEWED | Posted: 4 December 2023 doi:10.20944/preprints202312.0151.v1

cross-peak (multiplicity-sensitive gHSQCAD spectrum at 45 °C of the H-2 or H-3 proton (66.5 ppm and 65.97 ppm) of this fraction.

Given that the F1AP1 polysaccharide has a very high molar mass, it is expected to have increased aggregation, resulting in a main chain that adopts a compact coiled conformation.

3.1.3. NMR analysis of F1AP6 fraction of Apricot pectin

F1AP6 fraction was eluted by 0.2 M NaCl from DEAE Cellulose anion exchange column had a lower molecular weight that the previous samples, approximately 117.5 kDa (117.5 x 10^3 g/mol), therefore has more favorable t_2 relaxation rates than the previous F1AP and F1AP1 samples. This results in the observation of more peaks and narrower line shapes1, but the peaks are still too broad to retrieve coupling information. In the 2D-HSQC spectrum (Figure 11), 11 anomeric peaks are clearly observed.

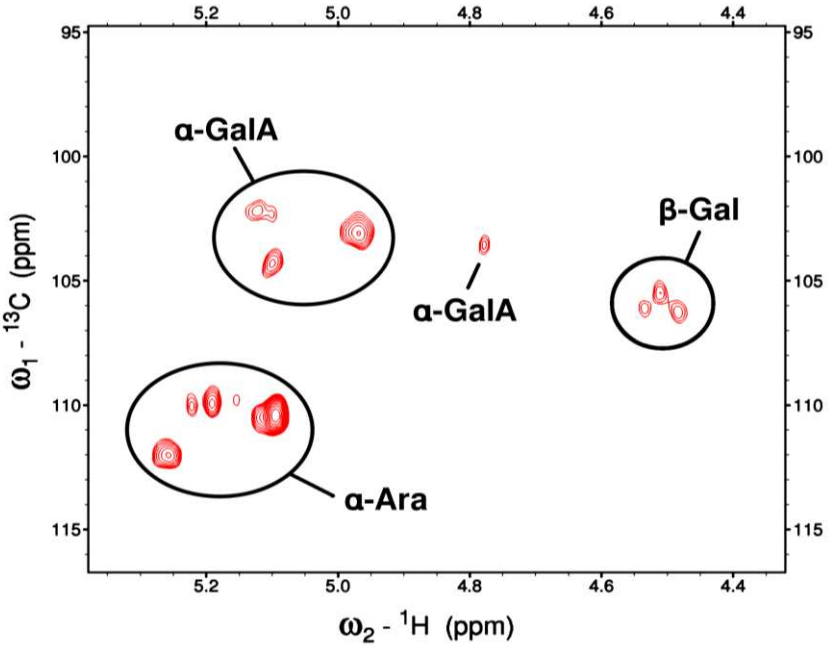

Figure 11. The HSQC anomeric region of F1AP6 at 45 °C.

The peaks at ~5.1-5.2 ppm in ^{1}H and ~110-112 ppm in ^{13}C were readily assigned as α-Ara based on their distinctive resonances. Similarly, the peaks at ~4.8-5.1 ppm in ^{1}H and ~102-104 ppm in ^{13}C were assigned as α-GalA. The weakest set of peaks, located at ~4.5/106 ppm (^{1}H/^{13}C), were assigned as β-Gal (t-, 4, and 6- linked) on the basis of both their chemical shifts and their weaker intensities, as expected from the monosaccharide analysis. A very weak anomeric peak is also observed at 4.78/103.5 ppm (^{1}H/^{13}C) but its identity could not be determined. In addition, two α-Rha sugars were identified on the basis of their C6 methyl resonances at ~1.26 / 19.5 ppm (^{1}H/^{13}C), each of which has COSY (Figure S4) and HMBC correlations to its own H5 at ~3.8-4.0 ppm and C5 at ~71-75 ppm.

As with the initial F1AP and F1AP1 samples, the α-Ara resonances have the strongest intensities because these sugars are in the more flexible side-chains, whereas the resonances of α-GalA, which resides in the more rigid backbone, are weaker than one might predict from the monosaccharide analysis alone.

The assigned ^{1}H and ^{13}C chemical shifts from the 2D NMR experiments at 45 °C are given in Table 6, and are based on through-bond correlations as well as comparisons to literature values for chemical shifts [24–26,41–45].

This is in agreement with previously published reports [11–15,25,26,38,40–43]. Using the HMBC and HSQCTOXY experiments, many of the other intra-residue resonances could be assigned for most of these sugars, but no inter-residue correlations could be reliably identified. The HMBC correlations reveal that one of the α -GalA is methyl esterified (3.82/55.67 ppm).

Preprints (www.preprints.org) | NOT PEER-REVIEWED | Posted: 4 December 2023 doi:10.20944/preprints202312.0151.v1

Table 6. Monosaccharide Assignments based on COSY, TOCSY, HSQC, HSQCTOXY and HMBC at 45 °C.

	C1	C2	C3	C4	C5	C6	H1	H2	H3	H4	H5	H6	Methyl Ester (H/C)
α-Rha	-	-	-	-	71.75	19.41	-	-	-	-	3.787	1.266	-
α-Rha	-	-	-	-	74.85	19.53	-	-	-	-	4.019	1.263	-
α-Ara	112.0	86.8	-	-	-	-	5.257	4.146	3.955	4.225	3.771, 3.726		-
α-Ara	109.9	-	79.5	-	-	-	5.159	4.138	3.911	4.216	3.939	-	-
α-Ara	110.5	-	-	-	64.16	-	5.112	4.143	3.971	4.235	3.838, 3.732		-
α-Ara	110.4	83.74	79.57	85.14	69.73	-	5.095	4.139	4.013	4.216	3.891, 3.805		-
α-Gal	106.1	-	-	-	-	-	4.534	-	-	-	-	-	-
α-Gal	105.5	-	-	-	-	-	4.511	-	-	-	-	-	-
α-Gal →6)-β-Galp-(1→	106.2	-	-	-	-	-	4.484	-	-	-	-	-	-
α-GalA	104.3	65.88, 77.14			74.22	-	5.106	3.802	3.789	4.146	4.706	-	-
α-GalA	102.1	-	-	-	73.26	173.4	5.118	4.15	-	-	5.08	-	3.817 / 55.67
α-GalA	103.0	-	-	-	-	-	4.968	3.737		"4.466	3.999"		-
α-GalA	103.5	-	-	-	-	-	4.779	-	-	-	-	-	-

The HSQC and HSQCTOXY experiments also indicate the presence of one methoxy group (3.358/51.85) and three acetyl groups was also observed at 1.96/22.97 ppm, 2.08/23.06, 2.186/23.36 with its carbonyl attachment at 183.2 ppm, 176.3 ppm and 176.4 ppm, respectively. The methyl and acetyl group $^{1}H/^{13}C$ NMR signals very closely correspond those observed for the F1AP1 fraction.

Thus, from comprehensive analysis of the isolation profile, monosaccharide composition, carbohydrate linkage, HPSEC, and 2D NMR results and literatures sources, we can conclude that the main pectin polysaccharides of the F1AP6 fraction of apricot fruits belong to backbone of repeats units of [-(1→4)-α-D-GalpA-1]n – both HG and partly contents RG-II polysaccharides, bearing heterosugar sidechains, including α-Ara, α -Rha and β-Gal residues. The observation of a carbonyl methyl ester in this fraction, identified by FTIR spectra (1740 cm-1) and by $^{1}H/^{13}C$ NMR (at 2.82/55.63 ppm) indicate that D-GalA residue in the HG regions of pectin is partly methylated. The DM was determined by FTIR to be 49.0%, which is lower than those of RG-I polysaccharide. Alternatively, RG-II residues might be attached to HG backbone with multiple complex side chains, as expected from the composition and carbohydrate linkage analysis, which can be cross-linked via borate diesters to the cell wall matrix [43].

These results are consistence with finding observed for the arabinose polymers the cell wall of some fruits, most likely arabinan and arabinogalactan in nature, [13,41,42]. The presence of RG-II connected to the HG chains in apricot pectin [46,47], shows the complexity and diversity in the structures of pectic polysaccharides greatly relate to the plant's origin and the extraction and isolation methods used [47]. Determining how they synthesis, interact with each other and how they are regulated Apricot fruits ripening is a tremendous challenge for the future.

4. Materials and Methods

4.1. Pectin hydrolysis-extraction and purification

Apricot fruits were obtained from local farms. Hydrolyze was performed by steam assisted flash extraction method [37] at temperature of 120 °C for 5 minutes. Pectin from these raw materials was extracted by DUF method [26]. To the swollen mass of apricot pomace residue (1700 g) a hydrochloric acid was added to adjust pH to 2.0.

 doi:10.20944/preprints202312.0151.v1

4.2. Determination of Molar mass by size exclusion chromatography

The sample solutions (2-5.0 mg/mL) were prepared by stirring at room temperature (20 °C) overnight. Each solution was filtered through a 0.45-µm syringe-driven filter (Millex HV, PVDF, Millipore Corp., Billerica, MA) before being characterized by HPSEC (1200 Series, Agilent Technologies, Santa Clara, CA). The solvent delivery system consisted of a vacuum degasser, autosampler, and a pump. The mobile phase was 50 mM $NaNO_3$ and 0.01% NaN_3 (pH 6.50). The injection volume was 200 µL, and the flow rate was held at 0.7 mL/min. Samples were run in triplicate. Two guard columns (TSK-GEL® PWXL 6.0 mm ID x 4.0 cm L, 12 µm, Tosoh Bioscience, Tokyo, Japan) were used. One was placed before the separation columns, which consisted of a set of three model TSK-GEL® PWXL size exclusion columns (7.8 x 300 mm, particle size 13 µ m, Tosoh Bioscience, Tokyo, Japan), and the other before the detectors. The column set was heated in a water bath at 35 ^{0}C and connected in series to a UV-1260 Infinity spectrophotometer (Agilent Technologies, Santa Clara, CA), HELEOS II multi-angle laser light scattering (LS) photometer (Wyatt Technology, Santa Barbara, CA), Model 255-V2 differential pressure viscometer (DP) (Wyatt) and an Optilab rEX-495 refractive index (RI) detector (Wyatt). Narrowly monodispersed pullulan P-50 (Shodex STANDARD P-82, JM Science, Grand Island, NY) was used to normalize the scattering intensity at the 90^0 angle. The percentage of recovery was obtained from the ratio of the mass eluted as determined by integration of the RI signal to the mass injected. All signals from the four detectors were analyzed by the ASTRA software (V.7.1.2.5, Wyatt Technology). The refractive index increment (dn/dc) values of 0.132 (mL/g) was used for mobile phase [37].

4.3. ATR-FTIR spectroscopy study of the Apricot pectin polysaccharides

The polysaccharide samples were dried at 110 ^{o}C for 30 min before analyzing by Fourier transform infrared (FTIR). Attenuated Total Reflectance FTIR (ATR-FTIR) spectra were acquired using a Thermo Scientific™ Nicolet™ iS50 FTIR spectrometer (Madison, WI, USA), which was equipped with a single bounce diamond crystal, a deuterated triglycine sulfate (DTGS) detector, and a potassium bromide (KBr) beam splitter. Samples were recorded in a scanning range 400–4000 cm^{-1} using 128 scans with a 2 cm^{-1} spectral resolution. A pressure control device ensured a good contact between the sample and the crystal. The background spectrum was acquired in air.

4.4. Glycosyl Uronic Acid Linkage Analysis

Methylation analysis was performed by slight modification of (Heiss, Stacey Klutts, Wang, Doering, & Azadi, 2009) [40]. The samples were prepared by weighing out 0.5 mg – 1 mg from each polysaccharide. The samples were treated with 400 µL of 0.5 M methanolic HCl for 20 min at 80°C and then dried with isopropanol. They were then reduced for 3 h with sodium borodeuteride ($NaBD_4$) in 100 mM ammonium hydroxide (NH_4OH) at room temperature. The $NaBD_4$ reduction solution was neutralized with acetic acid and removed by drying with methanol under N_2 atmosphere. Permethylation was affected by two rounds of treatment with sodium hydroxide (NaOH) base (30 min) and iodomethane (45 min). The sodium hydroxide base was prepared with 100 µL of 50 % NaOH, then 200 µL of methanol (MeOH) was added and vortexed together. Then 2 mL of dimethyl sulfoxide (DMSO) was added and the base solution was vortexed and centrifuged repeatedly up to 5 times to remove white residue which accumulates in NaOH base from its interaction with air. The supernatant of the base solution was removed which contains DMSO and the white residue. After the final wash, 2 mL of DMSO was added to the NaOH pellet and the solution was vortexed. 400 µL of the NaOH in DMSO base solution was added to each sample and then sonicated for 30 minutes. Then, 100 µL of iodomethane was added and the sample sat stirring at room temperature for 45 minutes. A second round of base and then iodomethane treatment was performed to ensure complete methylation.

Following sample workup, the permethylated material was hydrolyzed using 2 M TFA (2 h in sealed tube at 121 °C), reduced with $NaBD_4$ in 100 mM NH_4OH, and acetylated using 250 µL of acetic anhydride and concentrated trifluoroacetic acid (TFA). The sample was dried under a N2 stream and

 doi:10.20944/preprints202312.0151.v1

reconstituted in dichloromethane prior to injection on to the GC-MS. PMAA were analyzed on an Agilent 7890A GC interfaced to a 5975C MSD; separation was performed on a Supelco 2331 fused silica capillary column (30 m x 0.25 mm ID). The method is a derivation of the methylation linkage method reported by [40].

4.5. NMR spectroscopy methods

The sample was dissolved in D_2O with d_4-trimethylsilylpropanoic acid (TMSP) added as an internal reference standard. Its spectra were acquired on a 14 Tesla Agilent VNMRS NMR spectrometer (Santa Clara, CA) using a 5 mm OneNMR probe with z-axis pulsed field gradients. The F1AP1 sample was analyzed both at 45 °C and 80 °C, while the F1AP and F1AP6 sample were only analyzed at 45 °C. No significant differences were observed between the two temperatures.

The 1D-^{1}H NMR spectra were acquired with a 45° pulse angle, a relaxation delay of 1s and an 8 ppm spectral width, using 32k points and averaged over 64-256 transients. The 1D-^{13}C spectra were acquired with a 45° pulse angle, a relaxation delay of 0.2s and a spectral width of 220-250 ppm, using proton decoupling throughout, 32k data points and averaged over 30,000 – 100,000 transients.

The two-dimensional, gradient-enhanced, homonuclear correlation experiments, Constant-time COSY and zTOCSY were acquired with 7 ppm spectral widths in both dimensions, and averaged over 32-96 transients per acquisition, using 4k points in the directly-detected dimension and 256-512 indirectly-detected increments. The zTOCSY experiments were acquired using 100 ms and 22 ms mixing times. A series of NOESY experiments were acquired on the WSPF1 sample, using a range of mixing times ranging from 100 to 600 ms to observe the NOE buildup curve. These were acquired with a 7 ppm spectral width, averaging over 64 transients per increment and 400 indirectly detected increments. The 2D heteronuclear correlation experiments, HSQC and HSQCTOXY were gradient-enhanced and used adiabatic pulses. These spectra had a spectral width of 7 ppm in the directly-detected (^{1}H) dimension, while the indirectly detected dimension had 200 ppm and 70 ppm (centered at 85 ppm). The signal was averaged over 96-128 transients per increment, using 4k points in the directly-detected dimension and 256 indirectly-detected increments. The HSQCTOXY used mixing times of 100-120 ms. The HMBC experiment was acquired on the WSPF1 sample by averaging over 384 transients per increment, with 94 indirectly detected increments, and a spectral width of 70 ppm (centered at 85 ppm). The gradient enhanced HMBC also used adiabatic pulses, using 8, 10 and 12 Hz coupling constants, averaging over 128 transients per increment, and 280 increments in the indirectly detected dimension, The HMBC were acquired with a 140 ppm spectral width (centered at 120 ppm). All 2D spectra were processed using VNMRJ (Santa Clara, CA) and visualized using Sparky [24,45].

4.6. Statistical Analysis

All analyses were performed in triplicate, and the results were presented as mean values standard deviation. Data acquisition was done with the help of the Chromeleon Xpress software (Dionex, Thermo Scientific); Astra (20.0) software. The analysis of variance (ANOVA) was performed to identify significant differences ($p < 0.05$) among the samples were performed using Excel (Microsoft Office 2016).

5. Conclusions

The fine structure of pectin polysaccharides is discussed in this article from both literature and recent work we have performed on apricot pectin. The molar mass and hydrodynamic properties were determined by High Performance Size Exclusion Chromatography (HP-SEC) with DPV and RI detection. The monosaccharide compositions were determined by High-Performance Anion-Exchange Chromatography with Pulsed Amperometric Detection (HPAEC-PAD). Structural characterization utilized 1D and 2D homo- and hetero-nuclear NMR spectroscopy. The original fraction was found to be composed of D-galacturonic acid, L-rhamnose, D-arabinose and D-galactose in a 1.0 : 0.1 : 0.36 : 0.12 molar ratio, respectively, which is consistent with a pectin RG-1 branched

with arabinogalactan side chain polysaccharides, and has a weight-average molecular weight of approximately 1588.2 kDa. The slope of the hydrodynamic radius versus the molar mass was 0.57, indicating the presence of coil conformations.

The results from HPAEC-PAD, HPSEC and NMR spectroscopy (1H, 13C, zTOCSY, HSQC, HSQCTOXY and HMBC) demonstrated that fine fraction of F1AP1 has a backbone of (1→4)-linked -D-galacturonic acid and -L-rhamnopyranosyl residues branched with arabinogalactan side chains, having methyl and acetylated groups, and has high molecular weights. In contrast the other, F1AP6, fraction of apricot fruits belong to backbone of repeats units of [-(1→4)-α-D-GalpA-1]n – both HG and partly contents RG-II polysaccharides, bearing heterosugar sidechains, including α-Ara, α -Rha and β-Gal residues..

From our studies, the structure of F1AP1 mainly comprised of RG-I hairy regions with multiply glycosidic linkages of T- α-Araf, 3-α-Araf, 5-α-Araf, T- α -Arap, 2- α-Arap that constitute the side chains as an oligomer with different portions connected at the C-4 of rhamnosyl units in RG-I regions. The main symmetric and unimodal peaks of HPSEC (RI, LS and DP) were observed for F1AP1 with weight-average molecular weight of 1945 kDa and polydispersity index 1.91, demonstrating its high purity and homogeneity. The polysaccharide was highly viscosity and value of hydrodynamic reduce was 64,3 nm. The exponent b of Rh-Mw (conformation plot) are accepted to be 0.48 related to the compact flexible coil conformation of macromolecule in solution.

The β-configuration of all Galp units was inferred from their common chemical shifts of anomeric carbon (δ 103.40–104.22) and proton (δ 4.46–4.67) as presented in the anomeric region of HSQC spectrum. Presence of a carbonyl methyl ester in this fraction, identified by FTIR spectra (1740 cm-1) and by 1H/13C NMR (at 2.82/55.63 ppm) indicate that D-GalA residue in the HG regions of pectin partly methylated, the DM fined 49.0% is less than those of RG-I polysaccharide (74.5%). The F1AP6 polysaccharide has low molar mass (117 kDa), less aggregated and adopt more stiffness rod like conformation.

Supplementary Materials: The following supporting information can be downloaded at the website of this paper posted on Preprints.org. Figure S1: TIC chromatogram of the PMAA derivatives made from the F1AP sample; Figure S2: 1H and 13C NMR spectra: (a) F1AP; (b) F1AP1; (c) F1AP6; Figure S3: gCOSY (a) and Multiplicity-sensitive gHSQCAD spectrum of F1AP1 fraction at 80 °C; Figure S4: gCOSY and Multiplicity-sensitive gHSQCAD spectrum of F1AP6 fraction at 45 °C (green are CH2, red are CH and CH3).

Author Contributions: ZKM: Methodology, Investigation, Data interpretation and analysis, Writing—sections of the original draft; MHR: Methodology, Investigation; ASJ: Methodology, Data interpretation and analysis; JTB: Methodology, Data interpretation and analysis; GDS: Data interpretation and analysis, Writing—review, editing & revisions; LSL: Supervision, Conceptualization, editing & revisions. All authors have read and agreed to the published version of the manuscript.

Funding: This research received no external funding.

Data Availability Statement: The data presented in this study are available from the corresponding author upon request.

Acknowledgments: The authors would like to thank the ARS USDA for the support through the non-funding agreement # 58 8072 2 345 F, dated 9/2/2022. An analysis of monosaccharide composition was carried out with Dr. Arland Hotchkis and Dr. Hona Chau, whom the authors highly appreciated. We also gratefully acknowledge the methylation linkage analysis performed by the Complex Carbohydrate Research Center (Athens, GA USA), which was supported by the Chemical Sciences, Geosciences and Biosciences Division, Office of Basic Energy Sciences, U.S. Department of Energy grant (DE-FG02-93ER20097).

Conflicts of Interest: The authors declare no conflict of interest.

References

1. Bourguiba, H.; Scotti, I.; Sauvage, C.; Zhebentyayeva, T.; Ledbetter, C.; Krška, B.; Remay, A.; D'Onofrio, C.; Iketani, H.; Christen, D.; et al. Genetic Structure of a Worldwide Germplasm Collection of Prunus Armeniaca L. Reveals Three Major Diffusion Routes for Varieties Coming From the Species' Center of Origin. *Front Plant Sci* **2020**, *11*, 530439, doi:10.3389/FPLS.2020.00638/BIBTEX.

2. Huxley, A.; Griffiths, M.; Royal Horticultural Society (Great Britain) Dictionary of Gardening. **1992**.
3. Dragovic-Uzelac, V.; Levaj, B.; Mrkic, V.; Bursac, D.; Boras, M. The Content of Polyphenols and Carotenoids in Three Apricot Cultivars Depending on Stage of Maturity and Geographical Region. *Food Chem* **2007**, *102*, 966–975, doi:10.1016/J.FOODCHEM.2006.04.001.
4. Roussos, P.A.; Sefferou, V.; Denaxa, N.K.; Tsantili, E.; Stathis, V. Apricot (Prunus Armeniaca L.) Fruit Quality Attributes and Phytochemicals under Different Crop Load. *Sci Hortic* **2011**, *129*, 472–478, doi:10.1016/J.SCIENTA.2011.04.021.
5. Alajil, O.; Sagar, V.R.; Kaur, C.; Rudra, S.G.; Sharma, R.R.; Kaushik, R.; Verma, M.K.; Tomar, M.; Kumar, M.; Mekhemar, M. Nutritional and Phytochemical Traits of Apricots (Prunus Armeniaca L.) for Application in Nutraceutical and Health Industry. *Foods 2021, Vol. 10, Page 1344* **2021**, *10*, 1344, doi:10.3390/FOODS10061344.
6. Sochor, J.; Zitka, O.; Skutkova, H.; Pavlik, D.; Babula, P.; Krska, B.; Horna, A.; Adam, V.; Provaznik, I.; Kizek, R. Content of Phenolic Compounds and Antioxidant Capacity in Fruits of Apricot Genotypes. *Molecules* **2010**, *15*, 6285, doi:10.3390/MOLECULES15096285.
7. Dauchet, L.; Amouyel, P.; Hercberg, S.; Dallongeville, J. Fruit and Vegetable Consumption and Risk of Coronary Heart Disease: A Meta-Analysis of Cohort Studies. *J Nutr* **2006**, *136*, 2588–2593, doi:10.1093/JN/136.10.2588.
8. Ayour, J.; Sagar, M.; Alfeddy, M.N.; Taourirte, M.; Benichou, M. Evolution of Pigments and Their Relationship with Skin Color Based on Ripening in Fruits of Different Moroccan Genotypes of Apricots (Prunus Armeniaca L.). *Sci Hortic* **2016**, *207*, 168–175, doi:10.1016/J.SCIENTA.2016.05.027.
9. Tomás-Barberán, F.A.; Ruiz, D.; Valero, D.; Rivera, D.; Obón, C.; Sánchez-Roca, C.; Gil, M.I. Health Benefits from Pomegranates and Stone Fruit, Including Plums, Peaches, Apricots and Cherries. *Bioactives in Fruit* **2013**, 125–167, doi:10.1002/9781118635551.CH7.
10. Voragen, A.G.J.; Coenen, G.-J.; Verhoef, R.P.; Schols, H.A. Pectin, a Versatile Polysaccharide Present in Plant Cell Walls. *Struct Chem* **2009**, *20*, 263–275, doi:10.1007/s11224-009-9442-z.
11. Scheller, H.V.; Jensen, J.K.; Sørensen, S.O.; Harholt, J.; Geshi, N. Biosynthesis of Pectin. *Physiol Plant* **2007**, *129*, 283–295, doi:10.1111/J.1399-3054.2006.00834.X.
12. Burton, R.A.; Gidley, M.J.; Fincher, G.B. Heterogeneity in the Chemistry, Structure and Function of Plant Cell Walls. *Nat Chem Biol* **2010**, *6*, 724–732, doi:10.1038/NCHEMBIO.439.
13. Moore, J.P.; Farrant, J.M.; Driouich, A. A Role for Pectin-Associated Arabinans in Maintaining the Flexibility of the Plant Cell Wall during Water Deficit Stress. *Plant Signal Behav* **2008**, *3*, 102, doi:10.4161/PSB.3.2.4959.
14. Ha, M.A.; Viëtor, R.J.; Jardine, G.D.; Apperley, D.C.; Jarvis, M.C. Conformation and Mobility of the Arabinan and Galactan Side-Chains of Pectin. *Phytochemistry* **2005**, *66*, 1817–1824, doi:10.1016/J.PHYTOCHEM.2005.06.001.
15. Cornuault, V.; Posé, S.; Knox, J.P. Disentangling Pectic Homogalacturonan and Rhamnogalacturonan-I Polysaccharides: Evidence for Sub-Populations in Fruit Parenchyma Systems. *Food Chem* **2018**, *246*, 275–285, doi:10.1016/J.FOODCHEM.2017.11.025.
16. Khedmat, L.; Izadi, A.; Mofid, V.; Mojtahedi, S.Y. Recent Advances in Extracting Pectin by Single and Combined Ultrasound Techniques: A Review of Techno-Functional and Bioactive Health-Promoting Aspects. *Carbohydr Polym* **2020**, *229*, 115474, doi:10.1016/J.CARBPOL.2019.115474.
17. Roman-Benn, A.; Contador, C.A.; Li, M.W.; Lam, H.M.; Ah-Hen, K.; Ulloa, P.E.; Ravanal, M.C. Pectin: An Overview of Sources, Extraction and Applications in Food Products, Biomedical, Pharmaceutical and Environmental Issues. *Food Chemistry Advances* **2023**, *2*, 100192, doi:10.1016/J.FOCHA.2023.100192.
18. Frosi, I.; Balduzzi, A.; Moretto, G.; Colombo, R.; Papetti, A. Towards Valorization of Food-Waste-Derived Pectin: Recent Advances on Their Characterization and Application. *Molecules 2023, Vol. 28, Page 6390* **2023**, *28*, 6390, doi:10.3390/MOLECULES28176390.
19. Lara-Espinoza, C.; Carvajal-Millán, E.; Balandrán-Quintana, R.; López-Franco, Y.; Rascón-Chu, A. Pectin and Pectin-Based Composite Materials: Beyond Food Texture. *Molecules* **2018**, *23*, doi:10.3390/MOLECULES23040942.
20. Muhidinov, Z.K.; Bobokalonov, J.T.; Usmanova, S.R. *Pectin-Base for the Creation of a Functional Food*; Irfon: Dushanbe, 2019;

21. Peng, Y.; Zhang, Z.; Chen, W.; Zhao, S.; Pi, Y.; Yue, X. Structural Characterization, α-Glucosidase Inhibitory Activity and Antioxidant Activity of Neutral Polysaccharide from Apricot (Armeniaca Sibirica L. Lam) Kernels. *Int J Biol Macromol* **2023**, *238*, 124109, doi:10.1016/J.IJBIOMAC.2023.124109.
22. Cui, J.; Gu, X.; Wang, F.; Ouyang, J.; Wang, J. Purification and Structural Characterization of an α-Glucosidase Inhibitory Polysaccharide from Apricot (Armeniaca Sibirica L. Lam.) Pulp. *Carbohydr Polym* **2015**, *121*, 309–314, doi:10.1016/J.CARBPOL.2014.12.065.
23. Sun, W.; Labreche, F.; Kou, X. hong; Wu, C.E.; Fan, G.J.; Li, T.T.; Suo, A.; Wu, Z. Efficient Extraction, Physiochemical, Rheological Properties, and Antioxidant Activities of Polysaccharides from Armeniaca Vulgaris Lam. *Process Biochemistry* **2022**, *118*, 360–369, doi:10.1016/J.PROCBIO.2022.04.032.
24. Strahan, G.D.; Hotchkiss, A.T.; Dieng, S.; Hirsch, J. 1D and 2D NMR Datasets, Resonance Assignments and Coupling Constant Analysis of Red Beet Fiber and Pectin. *Data Brief* **2023**, *46*, 108845, doi:10.1016/J.DIB.2022.108845.
25. Hotchkiss, A.T.; Chau, H.K.; Strahan, G.D.; Nuñez, A.; Harron, A.; Simon, S.; White, A.K.; Yadav, M.P.; Yeom, H.W. Carrot Rhamnogalacturonan I Structure and Composition Changed during 2017 in California. *Food Hydrocoll* **2023**, *137*, 108411, doi:10.1016/J.FOODHYD.2022.108411.
26. Muhidinov, Z.K.; Ikromi, K.I.; Jonmurodov, A.S.; Nasriddinov, A.S.; Usmanova, S.R.; Bobokalonov, J.T.; Strahan, G.D.; Liu, L.S. Structural Characterization of Pectin Obtained by Different Purification Methods. *Int J Biol Macromol* **2021**, *183*, 2227–2237, doi:10.1016/j.ijbiomac.2021.05.094.
27. Muhidinov, Z. K., Bobokalonov, J. T., Ismoilov, I. B., Strahan, G. D., Chau, H. K., Hotchkiss, A. T., & Liu, L. Characterization of two types of polysaccharides from Eremurus hissaricus roots growing in Tajikistan. Food Hydrocolloids 2020, 105, 105768, https://doi.org/10.1016/j.foodhyd.2020.105768.
28. Lahaye, M.; Falourd, X.; Quemener, B.; Devaux, M.F.; Audergon, J.M. Histological and Cell Wall Polysaccharide Chemical Variability among Apricot Varieties. *LWT - Food Science and Technology* **2014**, *58*, 486–496, doi:10.1016/J.LWT.2014.04.009.
29. Filippov, M.P. Practical Infrared Spectroscopy of Pectic Substances. *Food Hydrocoll* **1992**, *6*, 115–142, doi:10.1016/S0268-005X(09)80060-X.
30. Coenen, G.J.; Bakx, E.J.; Verhoef, R.P.; Schols, H.A.; Voragen, A.G.J. Identification of the Connecting Linkage between Homo- or Xylogalacturonan and Rhamnogalacturonan Type I. *Carbohydr Polym* **2007**, *70*, 224–235, doi:10.1016/J.CARBPOL.2007.04.007.
31. Liu, X.; Renard, C.M.G.C.; Bureau, S.; Le Bourvellec, C. Revisiting the Contribution of ATR-FTIR Spectroscopy to Characterize Plant Cell Wall Polysaccharides. *Carbohydr Polym* **2021**, *262*, 117935, doi:10.1016/J.CARBPOL.2021.117935.
32. Ciriminna, R.; Fidalgo, A.; Delisi, R.; Tamburino, A.; Carnaroglio, D.; Cravotto, G.; Ilharco, L.M.; Pagliaro, M. Controlling the Degree of Esterification of Citrus Pectin for Demanding Applications by Selection of the Source. *ACS Omega* **2017**, *2*, 7991–7995, doi:10.1021/ACSOMEGA.7B01109/ASSET/IMAGES/AO-2017-01109E_M002.GIF.
33. Babkin, V.A.; Neverova, N.A.; Medvedeva, E.N.; Fedorova, T.E.; Levchuk, A.A. Investigation of Physicochemical Properties of Arabinogalactan of Different Larch Species. *Russ J Bioorg Chem* **2016**, *42*, 707–711, doi:10.1134/S1068162016070025/METRICS.
34. Zhou, X.L.; Sun, P.N.; Bucheli, P.; Huang, T.H.; Wang, D. FT-IR Methodology for Quality Control of Arabinogalactan Protein (AGP) Extracted from Green Tea (Camellia Sinensis). *J Agric Food Chem* **2009**, *57*, 5121–5128, doi:10.1021/JF803707A.
35. Kacuráková, M.; Capek, P.; Sasinková, V.; Wellner, N.; Ebringerová, A. FT-IR Study of Plant Cell Wall Model Compounds: Pectic Polysaccharides and Hemicelluloses. *Carbohydr Polym* **2000**, *43*, 195–203, doi:10.1016/S0144-8617(00)00151-X.
36. Fellah, A.; Anjukandi, P.; Waterland, M.R.; Williams, M.A.K. Determining the Degree of Methylesterification of Pectin by ATR/FT-IR: Methodology Optimisation and Comparison with Theoretical Calculations. *Carbohydr Polym* **2009**, *78*, 847–853, doi:10.1016/J.CARBPOL.2009.07.003.
37. Muhidinov, Z.; Teshaev, K.; Jonmurodov, A.; Khalikov, D.; Fishman, M. Physico-Chemical Characterization of Pectic Polysaccharides from Various Sources Obtained by Steam Assisted Flash Extraction (SAFE). *Macromol Symp* **2012**, *317–318*, 142–148, doi:10.1002/masy.201100108.
38. Phyo, P.; Wang, T.; Xiao, C.; Anderson, C.T.; Hong, M. Effects of Pectin Molecular Weight Changes on the Structure, Dynamics, and Polysaccharide Interactions of Primary Cell Walls of Arabidopsis Thaliana:

Insights from Solid-State NMR. *Biomacromolecules* **2017**, *18*, 2937–2950, doi:10.1021/ACS.BIOMAC.7B00888/SUPPL_FILE/BM7B00888_SI_001.PDF.

39. Fishman, M.L.; Cooke, P.H. The Structure of High-Methoxyl Sugar Acid Gels of Citrus Pectin as Determined by AFM. *Carbohydr Res* **2009**, *344*, 1792–1797, doi:10.1016/J.CARRES.2008.09.031.
40. Heiss, C.; Stacey Klutts, J.; Wang, Z.; Doering, T.L.; Azadi, P. The Structure of Cryptococcus Neoformans Galactoxylomannan Contains β-d-Glucuronic Acid. *Carbohydr Res* **2009**, *344*, 915–920, doi:10.1016/j.carres.2009.03.003.
41. Schols, H.A.; Posthumus, M.A.; Voragen, A.G.J. Structural Features of Hairy Regions of Pectins Isolated from Apple Juice Produced by the Liquefaction Process. *Carbohydrate Research : an international journal* **1990**, *206*, 117–129, doi:10.1016/0008-6215(90)84011-I.
42. Tan, L.; Zhang, L.; Black, I.; Glushka, J.; Urbanowicz, B.; Heiss, C.; Azadi, P. Most of the Rhamnogalacturonan-I from Cultured Arabidopsis Cell Walls Is Covalently Linked to Arabinogalactan-Protein. *Carbohydr Polym* **2023**, *301*, 120340, doi:10.1016/J.CARBPOL.2022.120340.
43. Caffall, K.H.; Mohnen, D. The Structure, Function, and Biosynthesis of Plant Cell Wall Pectic Polysaccharides. *Carbohydr Res* **2009**, *344*, 1879–1900, doi:10.1016/j.carres.2009.05.021.
44. Ulrich, E.L.; Akutsu, H.; Doreleijers, J.F.; Harano, Y.; Ioannidis, Y.E.; Lin, J.; Livny, M.; Mading, S.; Maziuk, D.; Miller, Z.; et al. BioMagResBank. *Nucleic Acids Res* **2008**, *36*, doi:10.1093/NAR/GKM957.
45. Goddard, T.D.; Kneller, D.G. SPARKY 3. University of California, San Francisco 2008.
46. Yapo, B.M. Pectic Substances: From Simple Pectic Polysaccharides to Complex Pectins—A New Hypothetical Model. *Carbohydr Polym* **2011**, *86*, 373–385, doi:10.1016/j.carbpol.2011.05.065.
47. Makarova, E.N.; Shakhmatov, E.G.; Belyy, V.A. Structural Studies of Water-Extractable Pectic Polysaccharides and Arabinogalactan Proteins from Picea Abies Greenery. *Carbohydr Polym* **2018**, *195*, 207–217, doi:10.1016/J.CARBPOL.2018.04.074.